




RESEARCH ARTICLE | JANUARY 01 2024

## Selective uptake and desorption of carbon dioxide in carbon honeycombs of different sizes **EP FREE**

N. V. Krainyukova  ; D. G. Diachenko; E. A. Kotomin 



*Low Temp. Phys.* 50, 97–102 (2024)

<https://doi.org/10.1063/10.0023898>



CrossMark



 **CryoComplete**

**A total solution for low-temperature characterization**

[Learn more >](#)



# Selective uptake and desorption of carbon dioxide in carbon honeycombs of different sizes



Cite as: Fiz. Nizk. Temp. **50**, 102–107 (January 2024); doi: [10.1063/10.0023898](https://doi.org/10.1063/10.0023898)

Submitted: 24 November 2023



View Online



Export Citation



CrossMark

N. V. Krainyukova,<sup>1,a)</sup> D. G. Diachenko,<sup>1</sup> and E. A. Kotomin<sup>2</sup>

## AFFILIATIONS

<sup>1</sup>B. Verkin Institute for Low Temperature Physics and Engineering of the National Academy of Sciences of Ukraine, Kharkiv 61103, Ukraine

<sup>2</sup>Institute of Solid State Physics, University of Latvia, Riga LV-1063, Latvia

<sup>a)</sup>Author to whom correspondence should be addressed: [krainyukova@ilt.kharkov.ua](mailto:krainyukova@ilt.kharkov.ua)

## ABSTRACT

Carbon honeycombs (CHs) are new carbon cellular structures, very promising in many respects, in particular, for high-capacity storage of various materials, especially in gaseous and liquid forms. In this study, we report a strong uptake of carbon dioxide kept inside carbon honeycomb matrices up to temperatures about three times higher as compared with CO<sub>2</sub> desorption at  $\approx 90$  K from flat solid surfaces in vacuum where we conduct our high-energy electron diffraction experiments. Desorption of CO<sub>2</sub> from CH matrices upon heating exhibits non-monotone behavior, which is ascribed to carbon dioxide release from CH channels of different sizes. It is shown that modeling of CO<sub>2</sub> uptake, storage, and redistribution in the thin CH channels of certain types and orientations upon heating can explain experimental observations.

Published under an exclusive license by AIP Publishing. <https://doi.org/10.1063/10.0023898>

## 1. INTRODUCTION

The era of graphite and diamond as the only two carbon forms known for thousands of years had finished in 1985 when the first fullerenes were discovered,<sup>1</sup> then followed by nanotubes,<sup>2</sup> schwarzites,<sup>3</sup> graphene,<sup>4</sup> and many other carbon forms, some of them are known only as theoretical predictions.<sup>5,6</sup> Several years ago, a new carbon allotrope called carbon honeycomb (CH) was first experimentally discovered by the author of this paper.<sup>7</sup>

Built from the carbon sheets known as graphene, CHs inherit some unique graphene properties, while, in contrast to graphene, they display not only the distinct 3D architecture but form stable cellular structures. Indeed, in all CHs the relatively wide but nano-sized channels are firmly connected and separated from each other by only one graphene layer. These are the first cellular structures in the carbon family, and their importance seems difficult to overestimate, first of all because all living forms on Earth are in fact carbon-based cellular systems. Initially, only one type of CH structures was suggested<sup>7,8</sup> to explain experimental observations, but it became clear later that at least two other structures should be considered depending of CH wall orientations and connection with each other.<sup>9,10</sup> In these structures, in particular, double adsorption of different species is possible as compared with graphene and carbon nanotubes due to the openness of both sides of the internal

graphene-like walls of cellular channels that offer unique potential for many energy-related applications, in particular for hydrogen storage.<sup>11</sup> Nowadays, along with the energy needs, equally important problem is to clean our environment from industrial and anthropogenic pollutants. One of such “pollutant” is carbon dioxide causing along with general harmful impact also gradual heating of the Earth atmosphere. CHs already demonstrated high capturing ability with respect to different gases including CO<sub>2</sub>.<sup>7,8,11–13</sup>

In our preliminary research,<sup>13</sup> we have found that the CO<sub>2</sub> uptake in CHs is very strong and the complete desorption of carbon dioxide captured in the carbon honeycomb matrix does not occur, even at high enough temperatures. This means that CHs used as membranes are very promising materials for CO<sub>2</sub> capturing. Moreover, we have found that desorption observed as the temperature function has a distinct two-stage character that was attributed to differently bonded CO<sub>2</sub> molecules with honeycomb walls, depending on channel configurations and sizes. Therefore, it was clear that the detailed analysis is needed, which allows for various CH models<sup>10</sup> with CO<sub>2</sub> molecules inside CH channels, desirably confirmed by the theory in order to elucidate the parameters of CO<sub>2</sub> capturing and release from CHs of certain configurations for potential applications. In this work, we suggest the study

of the carbon dioxide uptake in CHs observed in the experiment, undertaken to find the most plausible configurations presumably participating in the capture and release of CO<sub>2</sub> aiming to suggest their potentially controlled capture and further utilization.

## 2. EXPERIMENTAL METHODS

Carbon honeycomb samples in the form of thin films were prepared by the method of mild sublimation of graphene patches from thinned graphitic rods heated by the electric current flowing through these rods. Patches fly in a vacuum and then land on cleaved NaCl single-crystal surfaces. The first part of patches is deposited as upright standing graphene pieces on the NaCl surface since open chemical bonds around patch perimeters are highly unfavorable and tend to be closed.<sup>14</sup> The next portion of patches collides with the initially deposited fragments at high enough angles tending again to close the dangling bonds around graphene patches perimeters.<sup>10,15</sup> These processes are described in more detail in Refs. 7, 8, 10, and 11. The CH films obtained by the described method were separated from the salt substrates by means of dissolving of salt in distilled water and film floating with further capturing on the copper grid and putting on the sample holder inside the cryostat attached to the vacuum column of the electron diffraction setup.

In this work, as well as in many previous studies, we apply the high-energy electron diffraction method and use the specific structural approach, purposely developed for nanostructural materials. This approach is different as compared with the analysis typically applied to crystalline or amorphous materials. It is based on the use of a large set of structural models typically confirmed by theoretical calculations, in order to ensure their overall energetic stability. For all models, the diffraction curves are calculated applying the Debye formula<sup>16</sup> to be compared with the experimental diffractograms. The picture from the nanostructural objects typically may not be successfully described by a single structural model of a certain size. As a rule, some distributions are found over a few structural models comparable in their energetics and different in sizes. All reported here measurements are performed on the electron diffraction setup EMR-100 with the electron energy 50 keV supplied with the universal cryostat<sup>17</sup> filled in this study by liquid nitrogen. In this way, we can monitor not only the structure of our samples both pure CH matrices and CHs filled with CO<sub>2</sub> molecules but also processes occurring at different stages and temperatures.

In order to study any gas sorption in CHs, we developed and tested the specific procedure, enabled us to fill nearly fully all available positions inside CHs.<sup>7,8,10–12</sup> In this method, we first make deposition of gases at low temperatures below the known gas sublimation points, and then heat gradually our condensates till the temperatures 2–3 degrees lower these points and keep deposited gases at these temperatures for several minutes monitoring the electron diffraction patterns. Typically, the well-defined peaks from polycrystalline gas deposits disappear, but distinct residual signals left showing that some kind of composites based on CHs with sorbed gases form. In such processes, CO<sub>2</sub> molecules penetrate into CH matrices in a diffusive way by hopping between different positions on CH walls and junction lines. In more detail, this procedure will be illustrated in the next section. Our attempts to capture gases

from the gas phase at higher temperatures were unsuccessful apparently because of the high kinetic energy of molecules in the gas preventing their attachments to CH external surfaces.

## 3. RESULTS ON CO<sub>2</sub> UPTAKE AND DISCUSSION

In this study, we report carbon dioxide uptake in CH matrices and further desorption upon warming up to 230 K with relevant structural monitoring and analysis.

According to the general method of the CH matrix saturation by individual gases described in the previous section, we deposited CO<sub>2</sub> on prepared CH films in the vacuum column of the electron diffraction setup at 80 K (inside the cryostat cooled down to liquid nitrogen temperatures). At first, at the deposition temperature 80 K we see [Fig. 1(a)] the diffraction pictures typical of good quality polycrystalline crystals with the *Pa3* structure<sup>18</sup> with possible deviations of molecule orientations from cubic diagonals ascribed to their hopping precession about these diagonals as it was determined in Ref. 19. In Fig. 1 the contribution of the CH matrix [shown in the Inset of Fig. 1(a)] is subtracted. We also see that at warming the samples up to 90 K the polycrystalline peaks disappear but instead the strong broad signal at  $S \sim 1.9 \text{ \AA}^{-1}$  forms and is attributed to captured CO<sub>2</sub> molecules in CH channels. This signal at further warming to  $\sim 100 \text{ K}$  decreases and splits into two distinctly separate peaks numbered in Fig. 1, at higher temperatures these two separate peaks “interplay and compete”. The peak 2 gradually decreases from  $\sim 140$  to  $\sim 170 \text{ K}$  while the peak 1 first decreases from  $\sim 140$  to  $\sim 170 \text{ K}$  then it grows up. To uncover this puzzling behavior, we made the precise analysis of the diffraction patterns upon warming applying the simplified models for CO<sub>2</sub> uptake in the CH matrices.

## 4. STRUCTURAL MODELS FOR DENSE CARBON HONEYCOMBS AND HIGH TEMPERATURE CARBON DIOXIDE STORAGE INSIDE CH MATRICES

In the Inset of Fig. 1(a) one can see the typical diffraction pattern from carbon honeycomb matrices used in this work for CO<sub>2</sub> uptake. The peaks (100)Gr and (110)Gr are common for graphite as well as for graphene used as building blocks in CH structures. The relevant distances between carbon atoms are fully located inside graphene planes. But the first broad but distinct peak marked CH must fully belong to carbon honeycomb structures and is essentially shifted to smaller  $S$  as compared with the expected position at  $S \approx 2 \text{ \AA}^{-1}$  of the strongest peak (002) of graphite. Therefore, the CH structures, which have to contribute in this  $S$  range, have also to exhibit distinct peaks at such scattering wave vectors  $S$ .

On the other hand, one can reveal that the most noticeable signals from sorbed CO<sub>2</sub> in the CH matrices also located in the range of  $S \approx 1\text{--}2 \text{ \AA}^{-1}$ . Therefore, we can assume that CO<sub>2</sub> serves as intercalating material adjusted to the CH architecture in the thinnest channels and emphasizing the strongest peaks (100) and/or (110) typical of the hexagonal (as for the structures of the types A and C in Refs. 8 and 10) or pseudo-hexagonal (as for the structures of the type B in Ref. 10) ordered CH lattices. Moreover, some interesting hints can be found on the basis of consideration of the

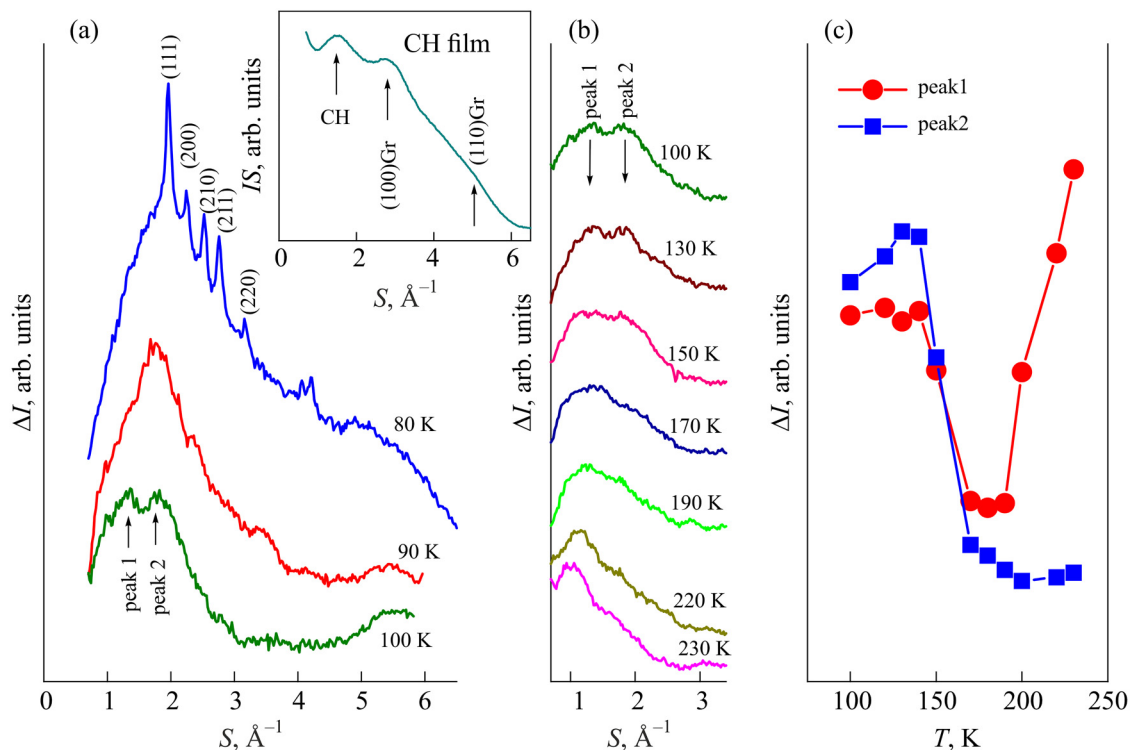


**FIG. 1.** Electron diffraction intensities from carbon dioxide sorbed in CH matrices as described in the text and warmed up to 230 K as functions of the scattering wave vector  $S = 4\pi \sin \theta / \lambda$ ,  $2\theta$  is the scattering angle and  $\lambda$  is the de Broglie wavelength of the electrons (a, b). The diffraction curve for the CH substrate [shown in the Inset in Fig. 1(a)] is subtracted. The maximal intensities of two peaks ascribed to sorbed  $\text{CO}_2$  in the different CH channels are shown in Fig. 1(c) vs temperature  $T$ .

diffraction pattern evolution with temperature (Fig. 1) and will be considered and discussed below.

Therefore within the big set of the model CH structures we chose only four structures shown in Fig. 2 with thinnest channels whose structural parameters correspond to the conditions described above, i.e., they may give the strong hexagonal (as for the A and C types of CHs) or pseudo-hexagonal (as for the B type) peaks in the relevant ranges of the diffraction patterns. Indeed, the detailed analysis of empty CHs showed that relative contributions of the densest CH structures in the total CH film structures were found to be about 35, 6, 8, and 14%, respectively, for the A1, A2, B1, and C0 structures shown in Fig. 2, the rest had wider channels. Allowing for this found distribution over sizes we made the next step, namely built and considered the simplified models of channels filled with  $\text{CO}_2$  molecules (Fig. 3) for all CH structures shown in Fig. 2. In these models all carbon dioxide molecule axes are perpendicular to the axes of the CH channels, aligned mainly towards the centers of hexagons in the CH walls or in a perpendicular direction, and layer by layer along the CH axes are arranged in an alternating cross-like manner. The flat molecular orientations in every layer along CH axes were chosen since such an arrangement may provide the densest channel filling allowing for the geometrical restrictions. Such models are simplified, the correct molecule locations and orientations can be

derived only from the precise theoretical considerations of varied configurations.

### 5. COMPARISON OF EXPERIMENTAL DIFFRACTOGRAMS WITH CALCULATED CURVES FOR SIMPLE MODELS OF CARBON DIOXIDE UPTAKE

The main contribution to the observed diffraction patterns from composites formed by CH matrices filled with  $\text{CO}_2$  molecules was found to give the structures with relatively thin channels (in total  $\sim 60\%$  or a little more). Only about 35–40% were shown to stem from CHs with the wider channels. These wide channels can be filled with  $\text{CO}_2$  molecules with more than one molecule located in one plane normal to the CH axes and occupied by molecules, therefore local molecule-molecule interactions could play an important role. In this case, the molecule arrangements in such wide channels may inherit some bulk-like features, stemmed in part from non-central quadrupole-quadrupole interactions between molecules.<sup>18</sup> For this reason it is natural to ascribe the first wide peak at low temperatures  $\sim 90$  K formed just after intensive diffusion of  $\text{CO}_2$  molecules inside CH matrices [Fig. 1(a)] to a dominant signal from the relatively large  $\text{CO}_2$  formations inside wider channels. This peak accordingly is centered closely to the positions of the most intensive bulk  $\text{CO}_2$  peaks and only slightly is shifted to

29 January 2024 12:54:48

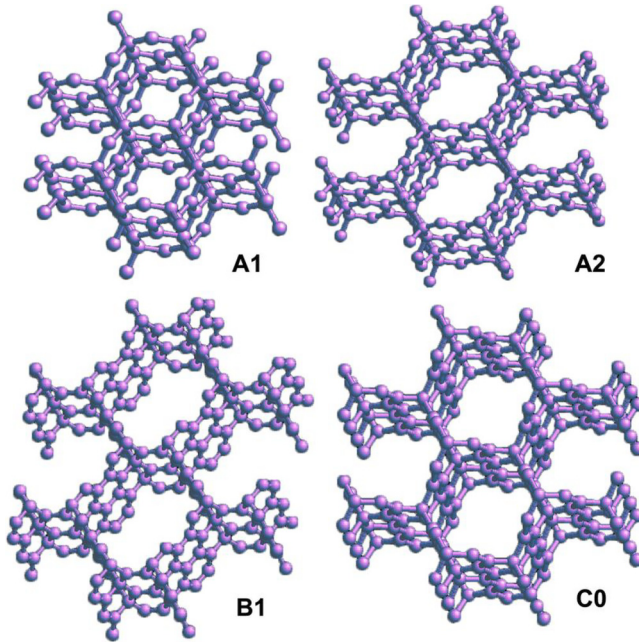


**FIG. 2.** Three types of the densest carbon honeycomb models A1, A2, B1, and C0 considered as the most plausible candidates for storing CO<sub>2</sub> in CHs at 120–230 K in vacuum.

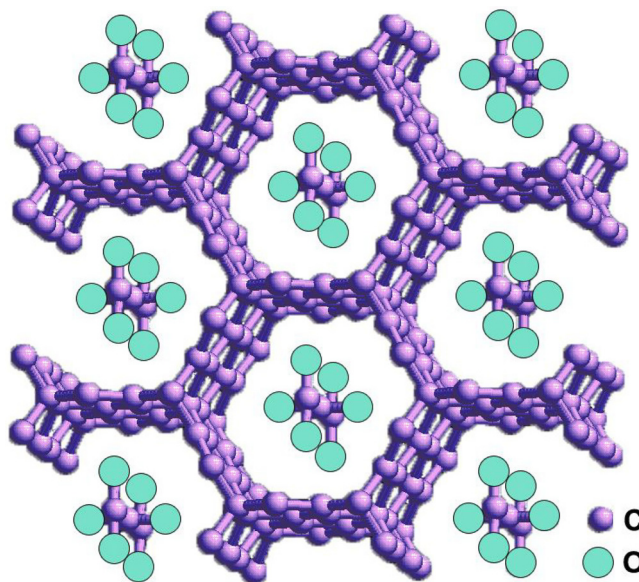


**FIG. 3.** Simplified model of carbon honeycomb of the A type filled with carbon dioxide molecules arranged along the channel axes in a cross-like manner from one horizontal level to the other along the CH axes. The similar arrangements of CO<sub>2</sub> molecules are considered for all other CH models shown in Fig. 2.

smaller  $S$  that can be ascribed to the orientational disorder causing the lattice expansion. This initial strong wide peak is well visible and dominant only at low enough temperatures and already at  $\sim 100$  K is replaced by less strong but still intensive double-peak signals. This double-peak part of diffractograms is most interesting for considering the high-temperature storage of CO<sub>2</sub>.

For calculations of anticipated diffraction patterns from carbon honeycomb matrices filled with carbon dioxide (Fig. 4) we applied the more complicated approach as compared with previous cases of pure CHs<sup>7,8,10,11</sup> allowing for two types of atoms A and B forming the diffraction patterns. As a type A, we consider carbon atoms regularly distributed not only in the carbon honeycomb matrices but also belonging to molecules of carbon dioxide while type B refers to oxygen atoms in CO<sub>2</sub> molecules. Then taking into account the general Debye formula for the intensity  $I$  in a cluster from  $N$  atoms<sup>16</sup>

$$I = \sum_{a,b}^N f_a f_b \frac{\sin(R_{ab}S)}{R_{ab}S}.$$

Here,  $R_{ab}$  are the distances between any two atoms  $a$  and  $b$  in a cluster,  $f_a$  and  $f_b$  are atomic scattering factors for electrons, we can calculate the total intensities

$$I_{A+B} = f_A^2 I_A + f_B^2 I_B + f_A f_B I_{AB},$$

where

$$I_A = N_A + 2 \sum_{l>k}^{N_A} \frac{\sin(R_{lk}S)}{R_{lk}S},$$

$$I_B = N_B + 2 \sum_{n>m}^{N_B} \frac{\sin(R_{nm}S)}{R_{nm}S},$$

and

$$I_{AB} = 2 \sum_{g>h}^{N_A+N_B} \frac{\sin(R_{gh}S)}{R_{gh}S} - 2 \sum_{l>k}^{N_A} \frac{\sin(R_{lk}S)}{R_{lk}S} - 2 \sum_{n>m}^{N_B} \frac{\sin(R_{nm}S)}{R_{nm}S}.$$

Factor 2 before the sums allows taking into account all atomic pairs only once;  $f_A$  and  $f_B$  are atomic scattering factors for electrons. The mean-square atomic displacements typically considered<sup>7,8,10,11</sup> are disregarded here since the  $S$  intervals are short.

Applying this approach we calculated diffraction patterns shown in Fig. 4(b) for four CH models A1, A2, B1, and C0 with thin channels and compared them with experimental observations shown in Fig. 1. The densest structure A1 (see also Fig. 2) was found not to be contributing in the double peak features either because these thinnest channels are not filled or their contribution can be found in other parts of diffraction patterns at smaller or larger  $S$  outside the considered  $S$  interval. But all three other model structures are certainly good candidates for comparison with experimental observations. The hexagonal structures A2 and C0 give distinct almost coinciding reflections (100) around peak 1 in the

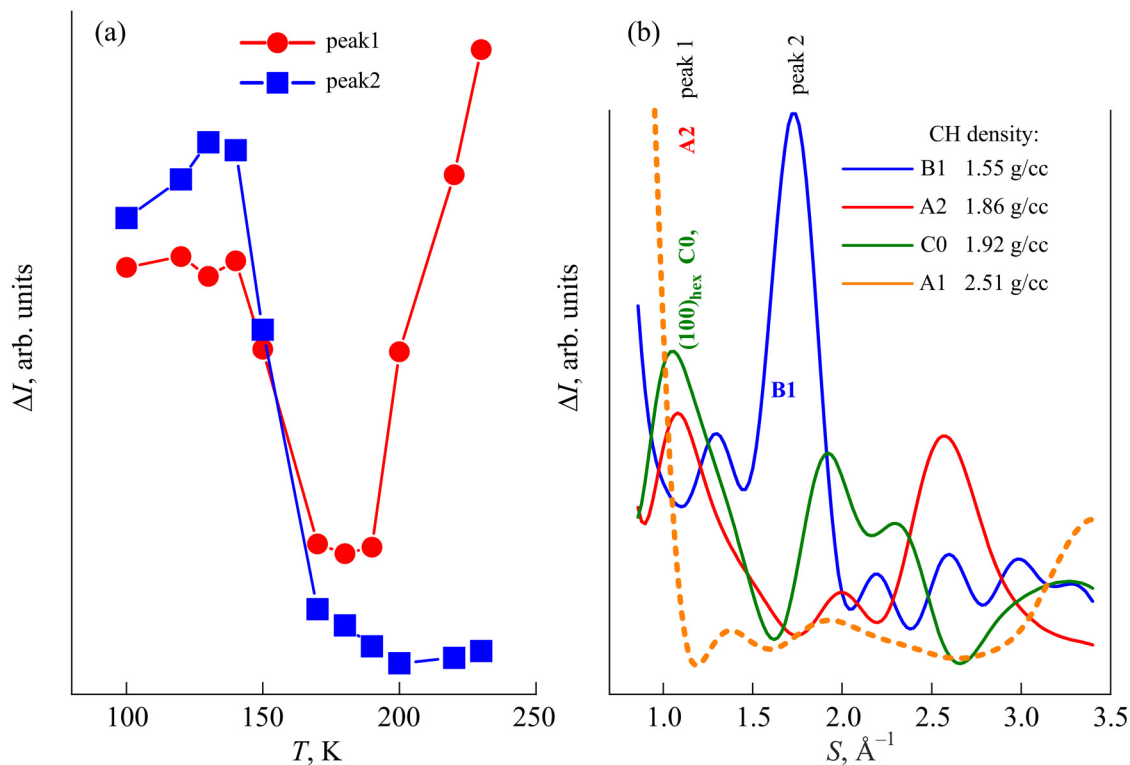


**FIG. 4.** (a) Temperature dependences of intensities of two separated diffraction peaks shown also in Fig. 1 with contribution of the CH film subtracted and (b) calculated diffraction patterns for CHs of certain configurations A1, A2, B1, C0 (with their densities  $\rho$ ) identified in Fig. 2 and filled by CO<sub>2</sub> as it is shown in Fig. 3.

experimental diffraction pattern in Fig. 1 while the big peak at  $S \approx 1.7 \text{ \AA}^{-1}$  belonging to the structure B1 well describes peak 2 observed in experiment in Fig. 1. We can also see a strong correlation between the carbon honeycomb densities and their ability to store larger or smaller amounts of gases depending on temperature. Indeed, our findings show that less dense CHs of the type B1 with a density of only 1.55 g/cc start to release CO<sub>2</sub> molecules at  $\approx 140 \text{ K}$  and are fully emptied from this gas at  $\approx 170 \text{ K}$ . The interesting feature observed here is the fact that the released gas can be successfully redistributed into the thinner channels (and denser structures) of A2 ( $\rho = 1.86 \text{ g/cc}$ ) and C0 ( $\rho = 1.92 \text{ g/cc}$ ) types and to be kept even at 230 K exhibiting the increase of the peak 1 above 190 K.

## 6. CONCLUSIONS

Applying the high energy electron diffraction and the specific carbon honeycomb preparation method, we have studied carbon dioxide uptake and release in the CH matrices. The advanced structural analysis enabled us to reveal a strong correlation between the sizes of the CH channels and the temperatures of this specific gas release that plausibly has more general character. In the thinnest channels of the structures A2 and C0 carbon dioxide can be kept even at temperatures about three times higher as compared with the sublimation point of this particular gas from a flat solid surface

in a vacuum, whereas from wider channels gas can be released at much lower temperatures.

Summing up, we have shown in this paper that carbon dioxide can be successfully captured in the CH channels from their solid deposited films in a vacuum if to perform gas condensation at  $\sim 80 \text{ K}$  applying liquid nitrogen for the holder cooling. Since vacuum conditions typically reduce the deposition temperatures for a wide class of classical gases by ca. 3 times we can expect that the same capturing mechanism can be realized at ambient pressures at almost room temperatures. This makes CHs good candidates for their use in cleaning atmosphere from this harmful gas. The further CO<sub>2</sub> release in this case may happen either by heating CH matrices with stored CO<sub>2</sub> to the higher temperatures or combining heating with pumping. Indeed, release is also important since collected CO<sub>2</sub> may be further used as renewable energy source by means of its transformation, e. g., into methane in the methanation reactions.<sup>20</sup>

## ACKNOWLEDGMENTS

The EK research was performed in the Center of Excellence of the Institute of Solid State Physics, University of Latvia, supported through European Unions Horizon 2020 Framework Programme H2020-WIDESPREAD-01-2016-2017-TeamingPhase2 under Grant Agreement No. 739508, Project CAMART2.

29 January 2024 12:54:48

## REFERENCES

- <sup>1</sup>H. W. Kroto, J. R. Heath, S. C. O'Brien, R. F. Curl, and R. E. Smalley, "C<sub>60</sub>: Buckminsterfullerene," *Nature* **318**, 162 (1985).
- <sup>2</sup>S. Iijima, "Helical microtubules of graphitic carbon," *Nature* **354**, 56 (1991).
- <sup>3</sup>T. Lenosky, X. Gonze, M. Teter, and V. Elser, "Energetics of negatively curved graphitic carbon," *Nature* **355**, 333 (1992).
- <sup>4</sup>K. S. Novoselov, A. K. Geim, S. V. Morozov, D. Jiang, Y. Zhang, S. V. Dubonos, I. V. Grigorieva, and A. A. Firsov, "Electric field effect in atomically thin carbon films," *Science* **306**, 666 (2004).
- <sup>5</sup>A. Hirsch, "The era of carbon allotropes," *Nat. Mater.* **9**, 868 (2010).
- <sup>6</sup>V. Georgakilas, J. A. Perman, J. Tucek, and R. Zboril, "Broad family of carbon nanoallotropes: Classification, chemistry, and applications of fullerenes, carbon dots, nanotubes, graphene, nanodiamonds, and combined superstructures," *Chem. Rev.* **115**, 4744 (2015).
- <sup>7</sup>N. V. Krainyukova, and E. N. Zubarev, "Carbon honeycomb high-capacity storage for gaseous and liquid species," *Phys. Rev. Lett.* **116**, 055501 (2016).
- <sup>8</sup>N. V. Krainyukova, "Capturing gases in carbon honeycomb," *J. Low Temp. Phys.* **187**, 90 (2017).
- <sup>9</sup>Z. Zhang, A. Kutana, Y. Yang, N. V. Krainyukova, E. S. Penev, and B. I. Yakobson, "Nanomechanics of carbon honeycomb cellular structures," *Carbon* **113**, 26 (2017).
- <sup>10</sup>D. G. Diachenko, and N. V. Krainyukova, "Structural variety and stability of carbon honeycomb cellular structures," *Fiz. Nizk. Temp.* **48**, 259 (2022) [*Low Temp. Phys.* **48**, 232 (2022)].
- <sup>11</sup>N. V. Krainyukova, B. Kuchta, L. Firlej, and P. Pfeifer, "Absorption of atomic and molecular species in carbon cellular structures (review article)," *Fiz. Nizk. Temp.* **46**, 271 (2020) [*Low Temp. Phys.* **46**, 219 (2020)].
- <sup>12</sup>N. V. Krainyukova, "Evidence for high saturation of porous amorphous carbon films by noble gases," *Fiz. Nizk. Temp.* **35**, 385 (2009) [*Low Temp. Phys.* **35**, 294 (2009)].
- <sup>13</sup>N. V. Krainyukova, Y. S. Bogdanov, and B. Kuchta, "Absorption-desorption of carbon dioxide in carbon honeycombs at elevated temperatures," *Fiz. Nizk. Temp.* **45**, 371 (2019) [*Low Temp. Phys.* **45**, 325 (2019)].
- <sup>14</sup>Q. Yuan, H. Hu, J. Gao, F. Ding, Z. Liu, and B. I. Yakobson, "Upright standing graphene formation on substrates," *J. Amer. Chem. Soc.* **133**, 16072 (2011).
- <sup>15</sup>T. Kawai, S. Okada, Y. Miyamoto, and A. Oshiyama, "Carbon three-dimensional architecture formed by intersectional collision of graphene patches," *Phys. Rev. B* **72**, 035428 (2005).
- <sup>16</sup>B. E. Warren, *X-Ray Diffraction* (Addison-Wesley, Reading, MA, 1969).
- <sup>17</sup>N. V. Krainyukova, V. O. Hamalii, A. V. Peschanskii, A. I. Popov, and E. A. Kotomin, "Low temperature structural transformations on the (001) surface of SrTiO<sub>3</sub> single crystals," *Fiz. Nizk. Temp.* **46**, 877 (2020) [*Low Temp. Phys.* **46**, 740 (2020)].
- <sup>18</sup>*Physics of Cryocrystals*, edited by V. G. Manzhelii and Yu. A. Freiman (American Institute of Physics, 1997).
- <sup>19</sup>N. Krainyukova, and B. Kuchta, "Hopping precession of molecules in crystalline carbon dioxide films," *J. Low Temp. Phys.* **187**, 148 (2017).
- <sup>20</sup>E. Billig, M. Decker, W. Benzinger, F. Ketelsen, P. Pfeifer, R. Peters, D. Stolten, and D. Thränae, "Non-fossil CO<sub>2</sub> recycling—The technical potential for the present and future utilization for fuels in Germany," *J. CO<sub>2</sub> Utiliz.* **30**, 130 (2019).